Journal of Engineering Mathematics **32:** 321–342, 1997.

The effect of solid conversion on travelling combustion waves in porous media

H. BYRNE* and J. NORBURY
Mathematical Institute, 24-29 St. Giles, Oxford OX1 3LB, U.K.

Received: 20 December 1994; accpeted in revised form: 7 October 1996

Abstract. A system of nonlinear partial differential equations, which describe the combustion of a gas passing through a porous medium, is examined. This model provides a bridge between recent porous-medium combustion studies and more classical combustion models. In particular, the effect of solid conversion on the downstream temperature is determined for travelling-wave solutions to the system. In cases for which the solid matrix is a perfect catalyst, solely enhancing the exothermic chemical reaction, with zero mass exchange, it is proved that the downstream temperature must always exceed the upstream temperature. However, when the solid is allowed to react with the gas, travelling-wave solutions for which the up- and down-stream temperatures are equal may be realised. A key result of this work is then the investigation of physical processes and related parameter ranges that give rise to travelling wave solutions with equal up- and down-stream temperatures. Specifically, two critical wavespeeds c_i with $0 < c_1 < c_2$ are identified. For $c < c_1$ the downstream temperature always exceeds that upstream, whilst for $c > c_2$ no bounded travelling-wave solutions exist. Behaviour in the region $c_1 < c < c_2$ is new: here solutions having equal up- and down-stream temperatures are realised. The two factors upon which this result depends are the inclusion into the model of solid conversion effects and the distinction between solid and gas temperatures. Thus the inclusion of a new physical process, that of heat storage in the solid varying as the reaction proceeds, allows the existence of a new type of travelling-wave solution.

Further phenomena studied include the appearance of nonunique solutions (which are of a type that may be related to ignition processes) and degenerate solutions which terminate precisely when all the solid and gaseous fuel is used up. Parameter regimes for the existence of these various types of solutions are found and the stability of such solutions discussed.

Key words: combustion, travelling-wave solutions, porous media.

1. Introduction

Throughout the last century a mathematical theory of combustion was developed to describe physical processes ranging from the oxidation of coal [1] to plug-flow chemical reactions [2] and frontal polymerization [3]. Analysis of such models has been made tractable by the exploitation of the large activation energies characteristic of combustion processes. Such activation-energy asymptotics effectively localise the chemistry, and associated heat production, in flames or (thin boundary) layers where the temperature remains approximately constant [4], [5], [6]. In such models travelling-wave solutions arise naturally to describe the steady propagation of the flame front, with the wavespeed and the outlet, or afterburn, temperature regarded as eigenvalues of the model equations. These eigenvalues then depend on system control parameters such as the inlet temperature, the inlet gas flux and the reaction temperature [4], [7], [8], [9], [10], [11].

Over the past fifteen years Norbury and co-workers have developed similar models [12], [13], [14], [15], [16], [17], [18], [19] which focus on combustion in porous media, as observed in, for example, automobile catalytic converters [20], filtration combustion [21], [22], the

* Mathematics Department, UMIST, PO BOX 88, Manchester M60 1QD, U.K.

burning of cigarettes [23], and the smouldering of polyurethane used to pad household furniture [24]. The resulting models differ from the 'classical' models in several ways. First, the solid and gas temperature are treated separately. In addition, the chemical and thermal properties of the solid change on combustion. Finally, for a porous medium, adoption of the high activation-energy asymptotics gives rise to a reaction zone of finite length in which the (dimensionless) temperature may exceed the critical reaction temperature by $O(1)$-fluctuations [12], [14], [16]. This contrasts with the classical case for which the reaction is localized at a front where the temperature makes asymptotically small fluctuations about the critical reaction temperature [4], [10].

To date, travelling wave analyses of models of porous-medium combustion have focussed on solutions for which the outlet temperature (u_{b}) is equal to the inlet temperature (u_{a}). This differs from classical analyses where, since heat is liberated by the chemical reaction, typically, $u_{\mathrm{b}} > u_{\mathrm{a}}$. One of the aims of this paper is, then, to identify those features of porous medium combustion which can give rise to solutions for which $u_{\mathrm{b}} = u_{\mathrm{a}}$. We can understand the practical importance of obtaining such a result by considering its implications for catalytic reactors used in industrial plants to treat harmful gases prior to their release into the atmosphere [25]. The existence of such solutions suggests that it may be possible to convert a gas containing harmful pollutants into a harmless gas which can be released into the atmosphere at the same temperature as the original noxious gas. A second, and potentially more hazardous, application is to household fires [24]. Here the existence of such solutions makes early detection of fires, on for example items of furniture, difficult because there is no discernible effect in the far-field, the solid and gas remaining at the ambient temperature there.

In this paper we consider a hybrid model which retains some of the distinguishing features of porous-medium combustion (namely two temperatures and solid conversion) whilst, at the same time, possessing a reaction rate more reminiscent of classical combustion models. Thus the chemical reaction is modelled by a delta function, localised on the combustion front, with (Heaviside) stepfunction factors to signify that the reaction can only be sustained when the solid temperature, gas concentration and solid-fuel concentration exceed critical values. This gives rise to two different types of solution: temperature-limited U-solutions which are characterised by the solid attaining the threshold reaction temperature at the combustion front; fuel-limited (Q,G)-solutions are characterised by solid fuel exhaustion behind the front and gas fuel exhaustion ahead of it. Degenerate solutions which are both temperature- and fuel-limited may also occur.

As mentioned above, through an analysis of this model we aim to bridge the gap between existing analyses of classical and porous-medium combustion models. In particular, we explain how separate treatment of the solid and gas temperatures, together with the inclusion of solid conversion effects, can give rise to travelling-wave solutions having equal up- and down-stream temperatures. Distinguishing between the solid and gas temperatures provides an effective heat-transfer mechanism between the two media. However, as the analysis of Section 4 demonstrates, this factor alone is not sufficient to establish equal up- and down-stream temperatures. Inclusion of a variable solid heat capacity is also necessary: the energy used to change the solid composition provides a sink for the energy produced by the chemical reaction. In this way, temperature growth may be restricted and equal up- and down-stream temperatures may result. The key result delimiting the existence of such solutions is summarised in the following theorem, which is proved in the text as a series of lemmas:

THEOREM 1. *Consider the class of travelling-wave solutions to Equations* (1)–(5)*, in which* μ *represents the gas mass flux,* λ *the solid heat capacity,* c *the wavespeed, whilst* u_{a} *and* u_{b} *represent the inlet and outlet temperatures. Defining critical wavespeeds* $c_1 = \mu$ *and* $c_2 = \mu + \lambda$*, then:*

(i) *all travelling-wave solutions with* $c < c_1$ *satisfy* $u_{\mathrm{b}} > u_{\mathrm{a}}$*;*
(ii) *there are no bounded travelling-wave solutions which have* $c > c_2$*;*
(iii) *for* $c_1 < c < c_2$ *travelling-wave solutions for which* $u_{\mathrm{b}} = u_{\mathrm{a}}$ *may occur.*

Nonuniqueness of travelling-wave solutions has been observed in a number of combustion models [4], [8], [7], [21], [22], the indeterminacy a consequence of an ill-defined wavespeed. Our hybrid model also admits nonunique travelling-wave solutions, the number of solutions depending on the range of wavespeeds under consideration. For example, when $c < \mu$, for each value of the system parameters only a finite number of travelling-wave solutions occur. This is demonstrated in Figure 4 where variation of the wavespeed c with the threshold reaction temperature u_{c} is sketched for a case in which the solid acts as a catalyst, unchanged in nature by the reaction (the inlet gas mass flux μ and the inlet temperature u_{a} are held fixed). With the solid acting as a catalyst, only temperature-limited U-solutions may occur. The resulting S-response curve, with one, two, or three nontrivial solutions depending on the value of u_{c}, is typical of combustion models [4]. For moderately low values of the threshold reaction temperature, a stable wave, which propagates towards the inlet, is established ($c > 0$). As u_{c} increases, the speed of this wave decreases in magnitude, changing direction when $c = 0$ and a standing wave occurs, until, as u_{c} passes through the turning point at $u_{\mathrm{c}} = u_{\mathrm{c}}^{\max}$, the solution branch loses stability. The system then jumps to the upper, stable branch. Such behaviour typifies the solution structure of the model when $c < \mu$. For most values of u_{c} a unique forward, or reverse, travelling wave occurs: the existence of multiple solutions is restricted to a finite range if $u_{\mathrm{c}} \in (u_{\mathrm{c}}^{\min}, u_{\mathrm{c}}^{\max})$.

By contrast, if $c > \mu$ a continuum of temperature-limited solutions, parameterised by the wavespeed are realised (temperature-limited solutions occur when the solid temperature becomes too low to sustain the reaction). Even when $u_{\mathrm{b}} = u_{\mathrm{a}}$ there is no unique solution. Such degeneracy has been observed by other authors [11], [26]. To select a unique solution they argue that, in practice, the solution which minimises the energy of the system will be realised – this corresponds to the minimum wavespeed.

The hybrid nature of the model we study means that in addition to temperature-limited solutions, solutions characterised by gas fuel and solid fuel exhaustion may also be realised. When such solutions are sought for wavespeeds $c > \mu$, a continuum of solutions is once more obtained (see Figure 7). However, each of the gas/solid fuel-limited solutions has a well-defined wavespeed: the degeneracy now concerns the ill-defined outlet temperature u_{b}. Future work, following the stability analysis outlined above, will determine which of these solutions would be observed in practice.

To summarise, we remark that only when $c_1 = \mu < c < \mu + \lambda = c_2$ are solutions for which $u_{\mathrm{b}} = u_{\mathrm{a}}$ attained. This statement is consistent with the results of Norbury and Stuart [17]. Using the same model and employing a standard porous-medium combustion reaction rate of finite strength which acts over a finite region, they obtained forward travelling-wave solutions for which $u_{\mathrm{b}} = u_{\mathrm{a}}$ when $c_1 < c < c_2$. An important difference between the results of [17] and those presented here is that we obtain *non-unique* solutions, parameterised by the wavespeed c for temperature-limited solutions and by the outlet temperature u_{b} for gas/solid fuel-limited solutions. This difference arises, we believe, in the limit as the finite-length,

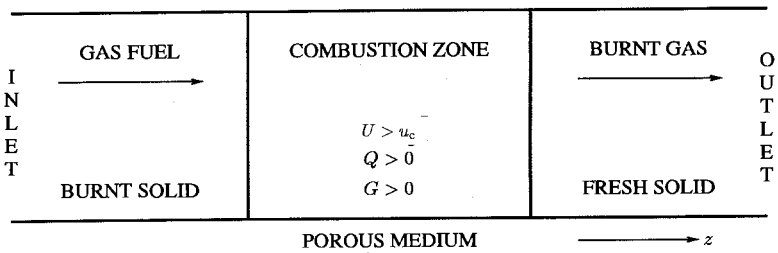

Figure 1. A schematic diagram of porous-medium combustion. A combustion zone propagates through the solid, in the same direction as the gas fuel, and separates a region containing fresh unburnt fuel from a region containing combusted exhaust gases.

finite-strength reaction rate approaches the delta function. In the limit, the distinct solutions obtained for the finite-length reaction rate coalesce, giving rise to a degenerate solution with a non-unique wavespeed. As mentioned above, indeterminacy of the wavespeed has been observed in other combustion models, see for example [11], [26]. Such degeneracy is unlikely to occur in practice; a time-dependent stability analysis should select from the admissible range a single wavespeed, namely that corresponding to the unique stable travelling wave, provided it exists. Future work will address this issue.

The outline of the paper is as follows. A brief description of the model of porous-medium combustion is presented in Section 2 whilst in Section 3 the travelling-wave model is developed. Sections 4 and 5 contain analysis of the travelling-wave model, commencing in Section 4 with the case for which the solid acts as a catalyst, chemically unaltered by the combustion process. For this case only solutions for which the upstream temperature (u_a) is less than the downstream temperature (u_b) can be realised. Further, only a finite number of nontrivial solutions occur. Solid conversion is re-introduced in Section 5 where we show that, for a prescribed range of gas velocities, solutions having equal up- and down-stream temperatures may now be realised (see Theorem 1). In addition, we obtain continua of travelling-wave solutions, which are characterised by the wavespeed for temperature-limited solutions and by the outlet temperature for gas/solid fuel-limited solutions. A limited stability analysis, contained in the Appendix, shows that both solid and gas fuel-limited solutions are stable with respect to a particular class of perturbations whereas, temperature-limited solutions are not.

2. Model description

In this section we present in nondimensionalised form the time-dependent, one-dimensional model of porous-medium combustion which we study: comprehensive derivations of the model can be found in [12], [14], [16] and [19]. The combustion process which we envisage, represented in Figure 1, involves the passage of a gaseous fuel, under pressure, through a porous medium in which combustion can occur. A combustion front propagates through the solid, in the same direction as the gas, and separates a region containing fresh, unburnt fuel from a region containing combusted exhaust gases. The model accommodates cases for which the solid acts as a catalyst for the reaction and also cases for which the solid reacts with the gas and is altered in chemical nature. Indeed, it is the inclusion of solid conversion that distinguishes this work from that of other authors ([7], [9]) in this area, giving rise to a richer solution structure which includes travelling waves having equal inlet and outlet temperatures.

The independent variables are z and t, whilst the dependent variables are the solid temperature $u(z,t)$, the gas temperature $w(z,t)$, the heat capacity of solid $\sigma(z,t)$ and the gas mass flux $g(z,t)$. The gas mass flux is proportional to the product of the gas temperature and the gas concentration. With reference to σ, we note that the solid comprises several materials, each with different heat capacities. As the reaction proceeds, fuel is consumed and the composition of the solid changes. In this way the solid heat capacity of the composite matrix also changes with time. In [19] Norbury and Stuart explain how and why the solid heat capacity and fuel concentration can be treated interchangeably: they derive a linear relationship between σ and the solid fuel concentration. Typically, as the solid is burned, the heat capacity of the composite solid also decreases.

The nondimensionalisation process introduces the (dimensionless) parameters (λ, μ, a) into the model. They have the following physical interpretations: λ is linearly related to the specific heat capacity of the solid; μ is proportional to the gas inlet velocity; a determines the ratio of the rate of gaseous consumption to that of the solid.

The model equations are presented below: Equations (1)–(2) derive from conservation of energy applied to the solid and gas fuels, respectively, whilst Equations (3)–(4) reflect mass conservation for the solid and gas fuels respectively.

$$\sigma\frac{\partial u}{\partial t} = \frac{\partial^2 u}{\partial z^2} + w - u + r, \qquad \frac{\partial w}{\partial z} = \frac{1}{\mu}(u - w), \tag{1, 2}$$

$$\frac{\partial \sigma}{\partial t} = -\lambda r, \qquad \frac{\partial g}{\partial z} = -\frac{a}{\mu}r. \tag{3, 4}$$

Here r denotes the reaction rate which is discussed below (see Equation (13)) and the parameters (λ, μ, a) are defined above. Heat transfer between the gas and solid is assumed to be proportional to the temperature difference $(u - w)$. The solid is consumed by an exothermic reaction at a fixed site in Equation (3), whilst the gas is rapidly transported through the reaction site by convection, so that $\partial/\partial t$-terms are absent in (2) and (4). We remark that, if all the solid fuel is consumed, then a matrix of residual combustion products remains to transport heat through the solid [14]. To close the system, the solid temperature is prescribed at both the inlet and outlet, while the gas temperature and gas flux are given at the inlet. Specifically, we impose

$$u(-\infty, t) = u_{\mathrm{a}} = w(-\infty, t), \qquad g(-\infty, t) = 1, \quad u(\infty, t) = u_{\mathrm{b}}, \tag{5}$$

where u_{a} and u_{b} are the ambient inlet and outlet temperatures. In addition, initial data, which determine, for example, $u(0,t)$ and $\sigma(0,t)$, must be specified.

Numerical solution of the above system of partial differential equations indicates that for certain initial data the system evolves to a quasi-steady state for which the burning zone propagates as a steady forward travelling wave [16]. When such solutions do not exist, it often indicates that the combustion dies out, with $u, w \to u_{\mathrm{a}} = u_{\mathrm{b}}$ as $t \to \infty$, and the reaction is no longer present. Depending on the choice of boundary conditions, there may also be unbounded increase of u, w in time. For example, if we prescribe $w(-\infty, t) = w_{\mathrm{a}} < u_{\mathrm{a}}$, then, from (2), we deduce that $\partial w/\partial z(-\infty, t) > 0$. We henceforth ignore such trivial or unbounded solutions and look for steadily propagating, nontrivial combustion waves. This assumption has been successfully employed in many combustion models, for example [10], [27]. Thus, we seek solutions which are functions of the single independent variable $x = z - ct$ where c is the constant wave velocity, to be determined as part of the solution.

3. Travelling-wave model

Introducing new dependent variables defined by

$$U(x) = u(z,t), \qquad W(x) = w(z,t), \qquad Q(x) = c\sigma(z,t), \qquad G(x) = g(z,t),$$

and using primes to denote differentiation with respect to $x = z - ct$, we may transform Equations (1)–(4) to give

$$0 = U'' + QU' + W - U + r, \qquad W' = \frac{1}{\mu}(U - W), \tag{6, 7}$$

$$Q' = \text{sign}(c)\lambda r, \qquad G' = -\frac{a}{\mu}r, \tag{8, 9}$$

subject to

$$U(-\infty) = u_{\text{a}} = W(-\infty), \qquad G(-\infty) = 1, \qquad U(\infty) = u_{\text{b}}. \tag{10}$$

In order to explain why Equation (8) is the correct formulation of Equation (3) when the model is transformed into travelling-wave coordinates, we argue as follows. In Equation (3) the time derivative balances the reaction rate. Whereas spatial derivatives always point in the same direction as derivatives of the travelling-wave coordinate x, time derivatives change direction as the sign of the wavespeed c changes. The factor $\text{sign}(c)$ is included into Equation (8) to ensure that the correct relationship between time derivatives and x-derivatives prevails for forward and reverse travelling waves ($c > 0$ and $c < 0$).

Assuming that the reaction is confined to a finite region, we deduce that the outlet solid concentration or, equivalently, the solid heat capacity remains constant. Thus, $\sigma(\infty)$ is constant ($\equiv 1$, by suitable scaling) and we impose

$$Q(\infty) = c, \tag{11}$$

where c is the unknown speed of the travelling wave. In addition, for bounded solutions at $x = \pm\infty$, it follows that

$$U'(\pm\infty) = 0. \tag{12}$$

Following [10], and to simplify the analysis, we assume, for the rest of this paper, that the chemical reaction takes place in a negligibly thin neighbourhood of the combustion front and can be modelled by a concentrated heat source located on the combustion front. Since this lies at $x = 0$ in the travelling-waave frame of reference, we set

$$r = \delta(x), \tag{13}$$

where $\delta(x)$ denotes the Dirac delta function. (Note that U, W are scaled so that $\int_{-\infty}^{\infty} r\,\mathrm{d}x = 1$, and that z, t are then scaled to obtain the coefficients shown in (1).) This assumption permits separate treatment of Equations (6)–(9) in the regions $x < 0$ and $x > 0$, subject to the following jump conditions:

$$[U] = 0 = [W], \qquad [U'] = -1, \qquad [Q] = \text{sign}(c)\lambda, \qquad [G] = -a/\mu, \tag{14}$$

where $[f] = f(0^+) - f(0^-) \equiv f^+ - f^-$ denotes the jump in any function f across $x = 0$. The first two conditions prescribe continuity of U and W across the front, whilst the remaining conditions, derived by integrating Equations (6), (8) and (9) across $x = 0$, specify the jumps in U', Q and G necessary to balance the reaction term. Note that if $Q^+ = c > 0$, then the jump condition for Q is $[Q] = \lambda$ whereas if $Q^+ = c < 0$, then the jump condition for Q becomes $[Q] = -\lambda$.

Recalling earlier models of porous-medium combustion [14], [16] and [19], and introducing u_c to describe the threshold reaction temperature, we assume further that each reaction is characterised by at least one of the following conditions:

- Solid-fuel limited $\Leftrightarrow Q^- = 0,\ G^+ \geqslant 0, U(0) \geqslant u_c$;
- Gas-fuel limited $\Leftrightarrow Q^+Q^- \geqslant 0,\ G^+ = 0, U(0) \geqslant u_c$;
- Solid-temperature limited $\Leftrightarrow Q^+Q^- \geqslant 0,\ G^+ \geqslant 0, U(0) = u_c$.

Before continuing, we emphasise that, when $Q^- = 0$, all solid fuel has been exhausted and the reaction is, therefore, extinguished. Even so, as we show in Equations (15)–(18), travelling-wave solutions can still occur. On the basis of the above classifications we now define the different types of solution which may be realised.

U-solutions occur when $Q^+Q^- \geqslant 0,\ G^+ \geqslant 0, U(0) = u_c$, with (Q,U)-solutions for the special case $Q^- = 0$, and (U,G)-solutions for the special case $G^+ = 0$;
(Q,G)-solutions occur when $Q^- = 0 = G^+, U(0) > u_c$;
Degeneracy occurs when $Q^- = G^+ = 0,\ U(0) = u_c$.

Using the above definitions, we now indicate how (λ, μ, a) parameter space may be partitioned into distinct regions in which nontrivial travelling-wave solutions exist. These results are summarised in Theorem 2:

THEOREM 2. *Consider the class of travelling-wave solutions to Equations* (1)–(5). *Solutions exist iff* $0 \leqslant \lambda \leqslant |c| = |Q^+|$ *and* $0 \leqslant a \leqslant \mu$, *with gaseous exhaustion occurring when* $a = \mu$, *solid exhaustion when* $|c| = \lambda$, *and temperature-limited solutions when* $0 \leqslant \lambda < |c|$ *and* $0 \leqslant a < \mu$. *For all other values of* λ, μ *and* a, $u \equiv w$ *and* $r \equiv 0$ *is the only possible solution.*

Proof. From (14) we observe that, where solutions exist, $|Q^+| = |c| = |Q^-| + \lambda \geqslant \lambda \geqslant 0$, with $|c| = \lambda$ when solid exhaustion occurs. Hence, for valid solutions we require $0 \leqslant \lambda \leqslant |c|$ with $|c| = \lambda$ when $Q^- = 0$.

Similarly, the jump in G across $x = 0$ supplies $G^+ = 1 - a/\mu \geqslant 0$ which is equivalent to $0 \leqslant a \leqslant \mu$, with $a = \mu$ when gaseous exhaustion occurs ($G^+ = -$).

Now, solid temperature-limited solutions occur when the parameters λ, μ and a remain feasible, that is, $0 \leqslant \lambda \leqslant |c|$ and $0 \leqslant a \leqslant \mu$. For any other parameter values no travelling-wave solutions occur. Further, inspection of the model equations shows that $u = w$ with $r = 0$ is then the only possible (bounded) solution. □

Since the parameter a enters the model only via the jump in G across the reaction front, we omit further discussion of a, assuming only that it takes values in the feasible range $a \in [0, \mu]$ and remarking that for the special case $a = \mu$ gaseous exhaustion occurs.

In the two regions $x < 0$ and $x > 0$ the model equations reduce to a system of linear ordinary differential equations which can be solved explicitly. These solutions are presented below.

$\underline{-\infty < x < 0.}$ In $-\infty < x < 0$, Equations (6)–(9) integrate to give

$$U = u_{\mathrm{a}} + A_1\,\mathrm{e}^{\alpha_1 x}, \qquad W = u_{\mathrm{a}} + A_1(1+\mu\alpha_1)^{-1}\,\mathrm{e}^{\alpha_1 x}, \tag{15, 16}$$

$$Q = Q^-, \qquad G = 1, \tag{17, 18}$$

where A_1 is a contant of integration and α_1 satisfies

$$0 = \alpha^2 + (Q^-/ + \mu^{-1})\alpha + (Q^-/\mu^{-1}). \tag{19}$$

Equation (19) has two real roots, one of which is negative. To ensure boundedness of solutions as $x \to -\infty$ this root is rejected: if both roots are negative (which corresponds to $Q^- > \mu$) then $A_1 = 0$ must be imposed also.

Conservation of energy ($x < 0$). For future use, we present here a result which expresses conservation of energy in $x < 0$ and can be derived by integrating Equation (6) once with respect to x (or by suitably rearranging Equations (15)–(18)):

$$U' + Q^- U - \mu W \equiv (Q^- - \mu)u_{\mathrm{a}}. \tag{20}$$

$\underline{0 < x < \infty.}$ In $0 < x < \infty$, Equations (6)–(9) integrate to give

$$U = u_{\mathrm{b}} + B_1\,\mathrm{e}^{\beta_1 x} + B_2\,\mathrm{e}^{\beta_2 x}, \tag{21}$$

$$W = u_{\mathrm{b}} + B_1(1+\mu\beta_1)^{-1}\,\mathrm{e}^{\beta_1 x} + B_2(1+\mu\beta_2)^{-1}\,\mathrm{e}^{\beta_2 x}, \tag{22}$$

$$Q = Q^+, \qquad G = G^+, \tag{23, 24}$$

where B_1 and B_2 are constants of integration and β_i $(i = 1, 2)$ satisfy

$$0 = \beta^2 + (Q^+\mu^{-1})\beta + (Q^+/\mu^{-1}), \tag{25}$$

with $B_i = 0$ if $\beta_i > 0$ to ensure boundedness of solutions as $x \to \infty$.

Conservation of energy ($x > 0$). Here conservation of energy is expressed thus:

$$U' + Q^+ U - \mu W \equiv (Q^+ - \mu)u_{\mathrm{b}}. \tag{26}$$

To fully determine the solution, conditions (14) and one of the reaction conditions must be imposed. Substitution with (15)–(18) and (21)–(24) evaluated at $x = 0^{\pm}$ supplies the following algebraic relations from which the constants A_1, B_1, B_2, G^+ and $Q^{\pm}$ may be determined.

$$u_{\mathrm{a}} + A_1 = u_{\mathrm{b}} + B_1 + B_2 \ (\equiv U(0)), \tag{27}$$

$$-1 = \beta_1 B_1 + \beta_2 B_2 - \alpha_1 A_1, \tag{28}$$

$$u_{\mathrm{a}} + A_1/(1+\mu\alpha_1) = u_{\mathrm{b}} + B_1/(1+\mu\beta_1) + B_2/(1+\mu\beta_2) \ (\equiv W(0)) \tag{29}$$

$$Q^+ = Q^- \pm \lambda, \qquad G^+ = 1 - a\mu^{-1}, \tag{30, 31}$$

$$G^+ = 0 \quad \text{or} \quad U(0) = u_{\mathrm{c}} \quad \text{or} \quad Q^- = 0. \tag{32}$$

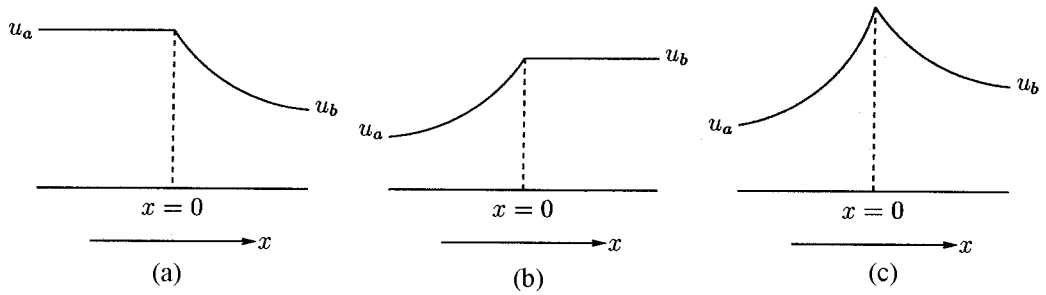

Figure 2. Typical solid temperature profiles for the model of porous-medium combustion: (a) the temperature maintains its inlet value $u_a \equiv u_c$ in $x < 0$ and decays exponentially to u_b ahead of the front (in $x > 0$); (b) the temperature increases from u_a to the constant value $u_c = u_b$ in $x < 0$ and maintains this fixed value ahead of the combustion front (in $x > 0$); (c) the temperature increases from u_a at the inlet to u_c at $x = 0$ and then decays exponentially to u_b ahead of the combustion front.

Conservation of energy ($-\infty < x < \infty$). Evaluating (20) and (26) at $x = 0^{\pm}$ and exploiting (28) and (29), we obtain the following equation, which is henceforth used in place of (29), and expresses conservation of energy over the whole domain ($-\infty < x < \infty$);

$$(Q^- - \mu)(u_b - u_a) = -1 + \lambda(U(0) - u_b)\,\mathrm{sign}(Q^+). \tag{33}$$

Thus Equation (33) corresponds to integration of (6), the equation governing conservation of solid energy, between $x = \pm\infty$. Further, setting $r = \delta(x)$ in the energy balance integral of Section 4 of [17] we recover Equation (33) for the special case $u_a = u_b$.

The form of the solution in $x < 0$ and $x > 0$ presented above leads now to a discussion of the possible types of reaction which may occur for different combinations of exponentials in $x < 0$ and $x > 0$ (see Figures 3(a)–(c)).

These include cases for which the solid and gas temperature are constant in $x < 0$ ($x > 0$) with exponential decay in $x > 0$ ($x < 0$) and are consistent with existing work, by, for example [10], for which the chemical system is assumed to be in thermal equilibrium. However, as shown in Figure 2(c), the appearance of decaying modes on both sides of the combustion front is different, arising because our model distinguishes between gas and solid temperatures.

- $U \equiv U(0)$ in $x < 0$. From Figure 2(a) we deduce that, if $U \equiv U(0) \geqslant u_c$ in $x < 0$, then solid exhaustion must occur there, so that $Q^- = 0$. Further, if $U(0) > u_c$ then we have a (Q,G)-solution and $G^+ = 0$ –, otherwise the reaction would continue in $x > 0$ until either the gas fuel was exhausted or the solid temperature fell below u_c. If $U(0) = u_c$, then we have a degenerate (U,Q)-solution.
- $U \equiv U(0)$ in $x > 0$. From Figure 2(b) we note that, since $U = U(0) \geqslant u_c$ in $x > 0$, $G^+ = 0$. Thus, possible solutions are (Q,G) and (U,G) solutions.
- $U \neq$ constant in $x < 0$ or $x > 0$. Referring to Figure 2(c), in this case, if $U(0) > u_c$ then a (Q,G) solution must occur. Otherwise, $U(0) = u_c$ and we have a U-solution.

Note that solutions for which $U \equiv$ constant are not permitted: they would violate (14).

Referring back to Equation (33), we now present a result relating the parameter λ to u_a and u_c for forward travelling waves when $u_a = u_b$.

LEMMA 1. *For forward travelling waves ($c > 0$), if $u_a = u_b$ then $U(0) = u_a + 1/\lambda$. Hence, when $u_b = u_a$, a necessary condition for the existence of such travelling-wave solutions is that λ be strictly positive and satisfy $u_a + 1/\lambda \geqslant u_c$*

The analogue of Lemma 1 for reverse travelling waves ($c < 0$) states that $u_c \leqslant U(0) = u_a - 1/\lambda < u_a$ when $u_b = u_a$. Hence, in this case, only (Q,G)-solutions are possible. However, as already stated in Theorem 1 and as Lemma 3 shows, $u_b > u_a$ for wavespeeds $c < \mu$ and, in particular, for $c < 0$. Thus no travelling-wave solutions for which $u_b = u_a$ and $c < 0$ can occur.

4. No solid conversion: $\lambda = 10$

In this section solutions for which the solid is chemically unaltered by the combustion process are studied: the solid acts as a catalyst with $\lambda = 0$, so that, from (33), $u_a \neq u_b$. It is, therefore, a digression from the key results regarding $u_a = u_b$ but yields useful approximations for the full model when λ is small, and provides the first example of degeneracy of the travelling-wave solutions to the model.

Setting $\lambda = 0$, we see that Equations (19), (25) and (30) supply

$$Q^+ = Q^- = c \Rightarrow \alpha_i = \beta_i \quad (i = 1, 2),$$

whilst (33) reduces to

$$(c - \mu)(u_a - u_b) = 1, \tag{34}$$

so that, as mentioned above, $u_a \neq u_b$. Recalling the definitions of α_i and noting that $0 \leqslant a \leqslant \mu$ and $0 = \lambda < |c|$, we deduce that the following cases may arise:

(a) $u_a > u_b \Leftrightarrow c > \mu \Rightarrow \alpha_1, \alpha_2 < 0$;

(b) $u_a < u_b \Leftrightarrow c < \mu \Rightarrow \alpha_2 < 0 < \alpha_1$.

Since for nontrivial solutions $|c| = |Q^{\pm}| > 0$, solid exhaustion cannot occur when $\lambda = 0$. Thus solutions having $U \equiv U(0)$ in $x < 0$ are not admissible (see Figure 2(a)), we reject case (a) henceforth, and Figure 2(c) depicts the qualitative nature of solutions when $u_a < u_b$. Solving Equations (27)–(29), (31) and (34) with $B_1 = 0$ and $U(0) = u_c$, we find the following expression relating u_c, u_a, u_b, μ and c:

$$u_c = \alpha_1 u_a - \alpha_2 u_b + 1/(\alpha_1 - \alpha_2) > u_a + 1/\alpha_1 - \alpha_2, \tag{35}$$

where α_1, α_2 are defined in terms of c and μ by Equation (19), and we have used the fact that $u_b > u_a$ to bound u_c below.

In practical situations, u_c is a constant, dependent on the solid (catalyst) and the composition of the inlet gases. Similarly, the system operating conditions determine the inlet gas velocity μ and the inlet temperature u_a. Thus, Equations (34) and (35) may be interpreted as defining c and u_b in terms of the control parameters μ, u_c and u_a. In Figures 4 and 5 variation of c and u_b with two of these parameters is sketched.

Figure 3 shows how c and u_b vary with μ for fixed values of u_a and u_c. From Figure 3(a) we note that, for small values of μ ($\mu < \mu^*$), a unique reverse travelling wave exists, whereas for larger values of μ ($\mu > \mu^*$), in addition to the reverse travelling wave, a pair of forward travelling waves exist. Thus the critical inlet gas velocity μ^* is a bifurcation point such that, as μ increases through μ^*, the number of travelling-wave solutions increases from one to three. From Figure 3(b) we note that larger wavespeeds give rise to larger outlet temperatures: this is consistent with (34) where, for fixed values of u_a and μ, $c_1 < c_2 < \mu$ implies that $u_{b1} < u_{b2}$.

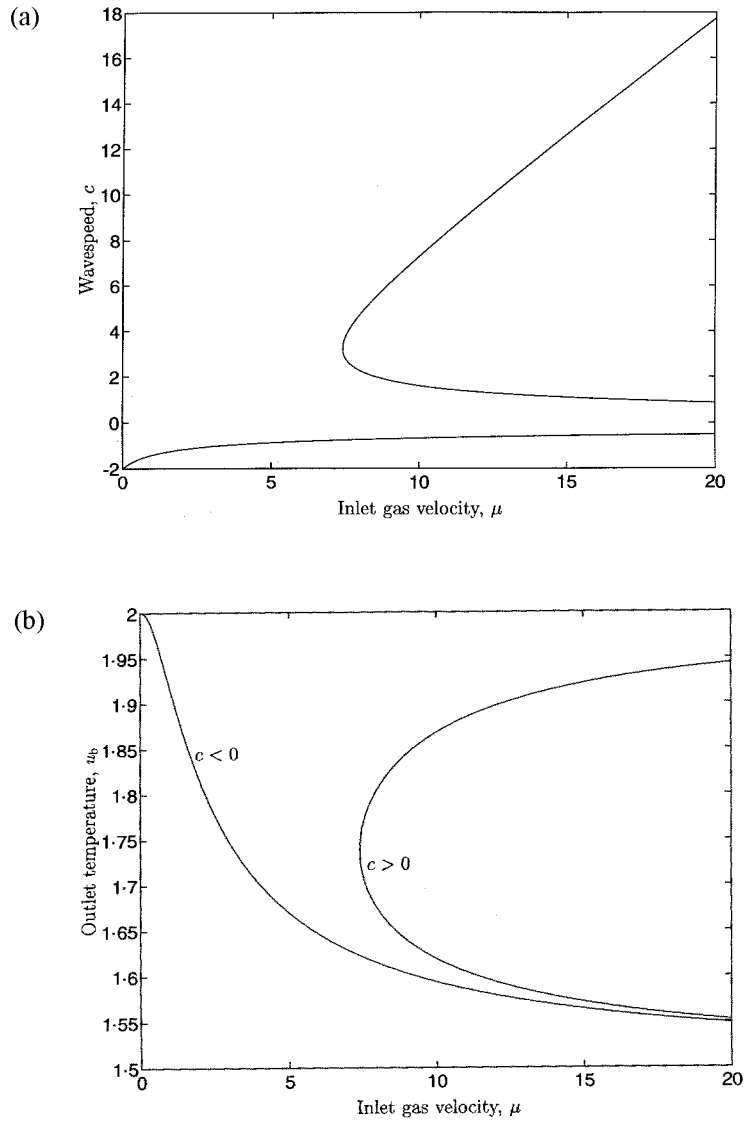

Figure 3. (a) Variation of the wavespeed c with the inlet gas velocity μ for a solid catalyst ($\lambda = 0$), holding the other control parameters, u_a and u_c, fixed. For all values of μ a reverse travelling wave exists. As μ increases, a critical inlet gas velocity is reached at which a unique forward travelling wave appears. For larger values of μ, in addition to the reverse travelling wave, there are two forward travelling waves. Parameter values: $\lambda = 0{\cdot}0$, $u_a = 1{\cdot}5$, $u_c = 2{\cdot}0$. (b) Variation of the outlet temperature u_b with μ. The profile shows how larger wavespeeds give rise to larger outlet temperatures. Parameter values as in Figure 3(a).

As $\mu \to \infty$ the two solution branches connect via a degenerate steady travelling wave having $c = 0$ and $u_b = u_a$.

In Figure 4 the variation of c and u_b with the threshold reaction temperature u_c is sketched. Now the existence of multiple solutions is restricted to a finite range of $u_c \in (u_c^{\min}, u_c^{\max})$, with a unique reverse travelling wave when $u_c < u_c^{\min}$, a unique forward travelling wave when $u_c > u_c^{\max}$, and three travelling waves for intermediate values of u_c. Variation of c and u_b with the inlet temperature u_a yields a diagram similar to Figure 4, except that increasing u_c is equivalent to decreasing u_a. We may see this by rewriting (35) in terms of $u_c - u_a$ and

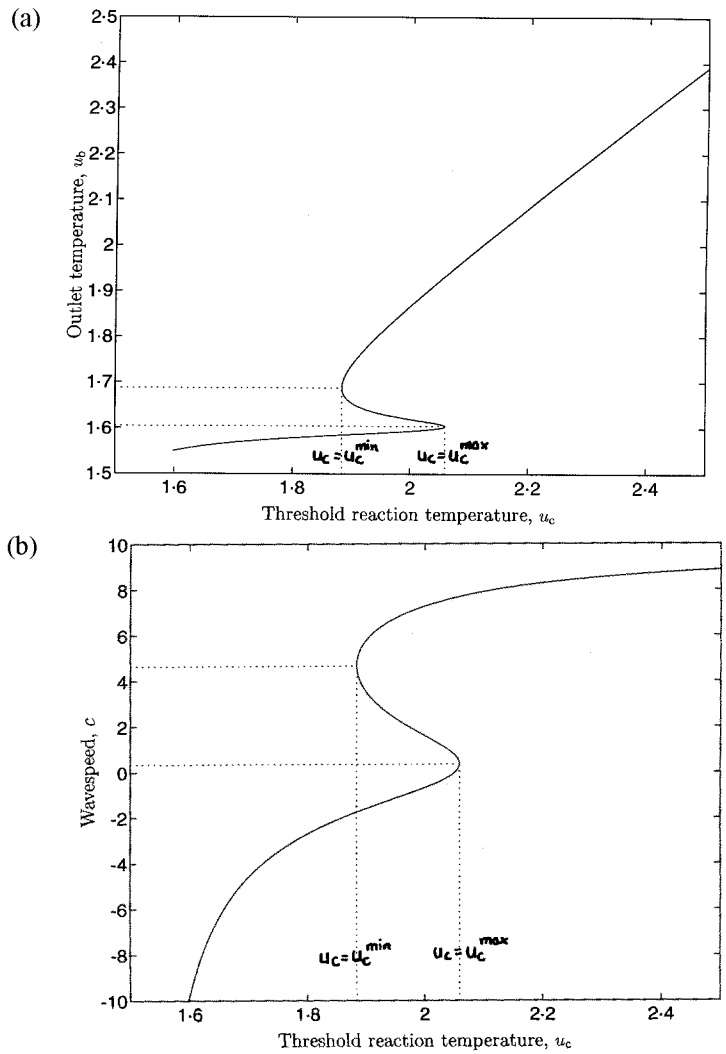

Figure 4. (a) Variation of the wavespeed c with the threshold reaction temperature u_c for a solid catalyst ($\lambda = 0$), holding the other control parameters, u_a and μ, fixed. The profile shows the existence of two critical threshold temperatures u_c^{min} and u_c^{max} such that when $u_c < u_c^{min}$ a unique reverse travelling wave occurs and when $u_c > u_c^{max}$ a unique forward travelling wave occurs. At $u_c = u_c^{min}$ a unique forward travelling wave appears. For $u_c \in (u_c^{min}, u_c^{max})$ three travelling-wave solutions exist. At $u_c = u_c^{max}$ two of the travelling-wave solutions coalesce, leaving a unique forward travelling wave when $u_c > u_c^{max}$. Parameter values: $\lambda = 0{\cdot}0, u_a = 1{\cdot}5, \mu = 10{\cdot}0$. (b) Variation of the outlet temperature u_b with u_c. Taken with Figure 4(a), the profile shows that the larger the wavespeed the larger the outlet temperature. Parameter values as in Figure 4(a).

$u_b - u_a$ or by rescaling (6)–(10), so that $U(-\infty) = 0 = W(-\infty), U(0) \geqslant u_c - u_a$ and $U(\infty) = u_b - u_a$. Both approaches show that it is the relative difference $u_c - u_a$ (and $u_b - u_a$) which is important, rather than their individual values, and also that increasing u_a has a similar effect on the model solutions as decreasing u_c.

Assuming that where a unique travelling wave exists it is stable and that the stability of a branch of solutions changes as a fold point is traversed, we may use Figure 4 to explain how a stable, forward travelling wave is established in a practical situation. Initially, for moderate values of u_c, a stable travelling wave, which propagates towards the inlet, is established. As

u_c increases beyond the turning point at $u_c = u_c^{\min}$, this wave loses stability, the system jumps to the upper solution branch and a stable, forward travelling wave is realised. This behaviour describes the lightoff phenomena observed experimentally in catalytic converters [28].

5. Inclusion of solid conversion: $\lambda > 0$

In this section we demonstrate how, by allowing Q (and hence the solid heat capacity, σ) to vary, solutions for which $u_b = u_a$ may be realised for a particular range of wavespeeds. The two features of our model crucial in obtaining this result are the separate treatment of the solid and gas temperatures and the inclusion of solid conversion effects, these factors giving rise to a single exponential mode in $x < 0$ and (at most) two exponentials in $x > 0$. In addition, by relaxing the constraint $u_b = u_a$, we are able to show that, in fact, there exists a family of degenerate (Q,G)-solutions, characterised by the outlet temperature u_b. This result is new: other analyses have reported the existence of families of travelling-wave solutions characterised by the wavespeed c, and not u_b [11].

Recalling the definitions of α_i and β_i we deduce that, when $\lambda > 0$, the following cases may arise:

(A) $\mu > Q^+$, $\mu > Q^-$ and $Q^+Q^- \geqslant 0$;

(B) $Q^+ > \mu > Q^- \geqslant 0$.

The case $Q^+ > Q^- > \mu > 0$ is not considered since, from an argument similar to that used in Section 4, no solutions exist when $Q^- > \mu$. Cases (A) and (B) are possible and are discussed, in turn, below.

CASE (A): $\mu > Q^+$, $\mu > Q^-$

In this case there are decaying modes in $x > 0$ and $x < 0$, so that, referring to Figure 2(c), both (Q,G) and U-solutions are possible.

(Q,G)-solutions. With $Q^- = 0 = B_1$, and

$$Q^+ = c = \pm\lambda < \mu \tag{36}$$

Equations (27)–(33) yield the following expression for u_b:

$$u_b = u_a - (\alpha_1 - \beta_2 - c)/(\mu\beta_2 - \mu\alpha_1 + c\alpha_1). \tag{37}$$

If we regard λ, μ, u_c and u_a as the control parameters, Equations (36) and (37) define the wavespeed c and the outlet temperature u_b in terms of the system parameters. Thus, as in Section 4, the dependence of c and u_b on λ, μ, u_c and u_a can be assessed. For example, Figure 5(a) depicts the variation of u_b with the solid heat capacity λ.

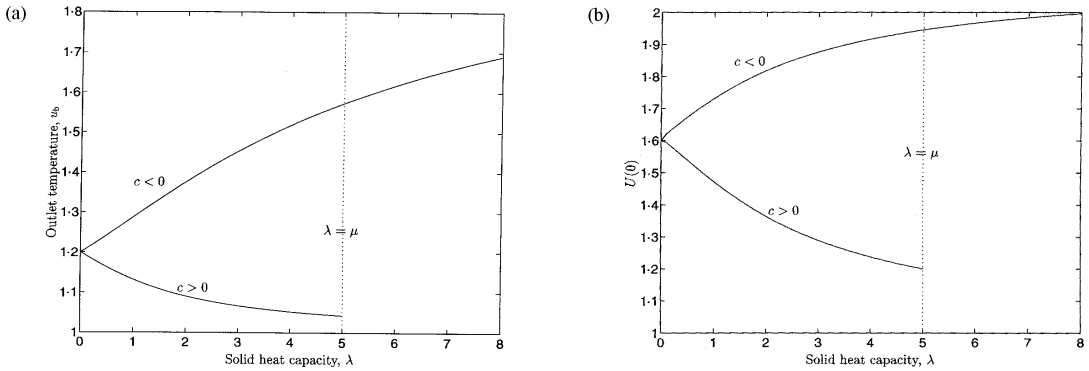

Figure 5. (a) Variation of u_b with the solid heat capacity λ for (Q,G)-solutions, holding u_a, u_c and μ fixed. The profile shows that where $0 < \lambda < \mu$ both forward and reverse travelling wavs exist, whereas when $\lambda > \mu$ only the reverse travelling wave persists. Further, the reverse travelling-wave solutions give rise to larger outlet temperatures. Parameter values: $u_a = 1{\cdot}0$, $u_c = 1{\cdot}2$, $\mu = 5{\cdot}0$. (b) Variation of $U(0)$ with λ. The profile shows that the maximum solid temperature occurs at $x = 0$. Parameter values as in Figure 6(a).

From the diagram we note that for $0 < \lambda < \mu$, two travelling-wave solutions exist whereas for $\lambda > \mu$ only the reverse travelling wave for which $c = -\lambda < \mu$ exists. Where two solutions exist, the forward travelling wave gives rise to a lower outlet temperature. This contrasts with the (U,U) solutions discussed in Section 4 where $\lambda = 0$ (see Figures 4 and 5). We remark also that, where solutions exist, the inequality $u_b > u_a$ is once again maintained, a result proved below in Lemma 2. For valid solutions, we must ensure that $U(0) > u_c$. Having determined u_b from (37), we substitute in Equation (33) to obtain

$$U(0) = u_b + \lambda^{-1}\,\mathrm{sign}(c)\{1 - \mu(u_b - u_a)\}.$$

In Figure 5(b) the variation of $U(0)$ with respect to λ is sketched where we have used the parameter values adopted in Figure 5(a).

LEMMA 2. *All (Q,G)-solutions for which $c < \mu$ satisfy $u_b > u_a$.*

Proof. Since $\beta_2 < 0 < \alpha_1$ and $c < \mu$, we deduce that

$$\mu\beta_2 - \mu\alpha_1 + c\alpha_1 = \mu\beta_2 - (\mu - c)\alpha_1 < 0.$$

Further, substitution with α_1 and β_2 from Equations (19) and (25), and setting $Q^- = 0$, supplies

$$\alpha_1 - \beta_2 - c = (\mu^{-2} + 4)^{1/2} + [(c + \mu^{-1})^2 + 4(1 - c/\mu)]^{1/2} - c > 2/\mu > 0,$$

where we have exploited the fact that $c < \mu$. Combining these two results in Equation (37), we complete the proof. □

U-solutions. With $U(0) = u_c$ and $B_1 = 0$, Equations (27)–(33) are seen to supply the following pair of expressions which define c and u_b in terms of the control parameters λ, μ, u_c and u_a:

$$u_b - u_a = \frac{u_c - u_a}{1 + \mu\alpha_1} + \frac{1 - \alpha_1(u_c - u_a)}{\beta_2(1 + \mu\beta_2)}, \tag{38}$$

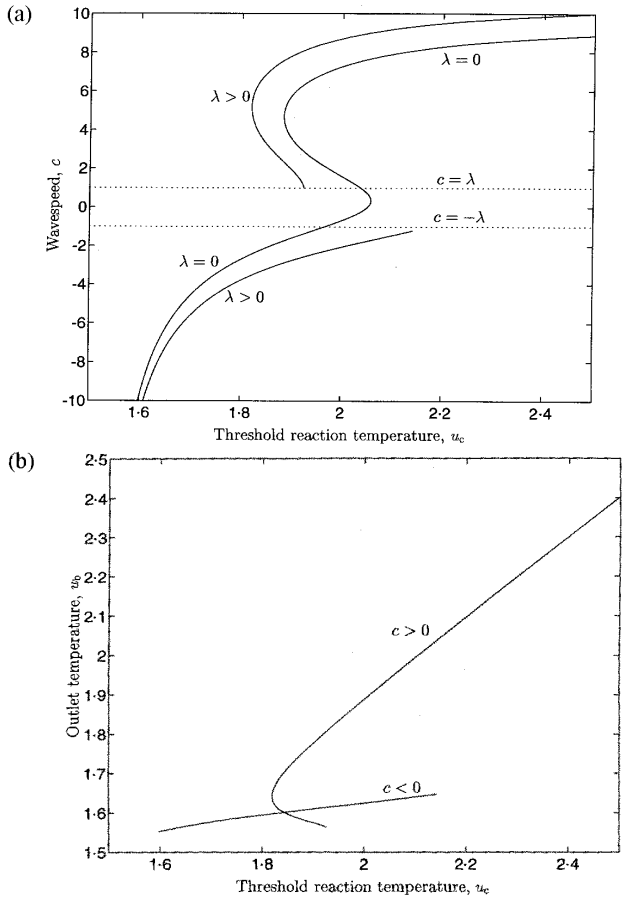

Figure 6. (a) Variation of c with u_c for U-solutions, holding μ, u_a and $\lambda > 0$ fixed. (The (u_c, c)-curve for the case $\lambda = 0$ is included for comparison.) The profile shows the existence of u_c^{min} and u_c^{max} such that for $u_c < u_c^{min}$ a unique reverse travelling wave occurs and for $u_c > u_c^{max}$ a unique forward travelling wave occurs. In the intermediate region, the condition $|c| < \lambda$ leads to the appearance of a third critical temperature u_c^{int} such that for $u_c \in (u_c^{min}, u_c^{int})$ three travelling-wave solutions exist whilst for $u_c \in (u_c^{int}, u_c^{max})$ only two travelling-wave solutions exist. Parameter values: $\lambda = 5{\cdot}0, \mu = 10{\cdot}0, u_a = 1{\cdot}0$. (b) Variation of u_b with u_c. Parameter values as in Figure 6(a).

$$u_b = \frac{\lambda u_c - \text{sign}(c)[1 - (Q^- - \mu)u_a]}{\lambda + \text{sign}(c)(Q^- - \mu)}, \tag{39}$$

where α_1, β_2 are defined in terms of $Q^{\pm}, \lambda$ and μ by Equations (19) and (25), whilst $Q^{\pm}$ are related by Equation (30). Variations of c and u_b with respect to u_c are sketched in Figure 6. For comparison with the analysis of U-solutions presented in Section 4, the variation of c with u_c in the case $\lambda = 0$ is also included in Figure 6(a).

From the figures, we note, once again, that $u_b > u_a$ for all travelling-wave solutions, a result which we prove below in Lemma 3.

LEMMA 3. *All U-solutions for which $c < \mu$ satisfy $u_b > u_a$.*

Proof. Combining Equations (27) and (29) with $B_1 = 0$ and $U(0) = u_c$, we deduce that

$u_b - u_a = (u_c - u_a/(1 + \mu\alpha_1) - (u_c - u_b)/(1 + \mu\beta_2)$.

Rearranging (25) and using the inequality $\beta_2 < -(c + 1/\mu)$, we deduce that

$$(1 + \mu\beta_2)^{-1} = (c + \beta_2)/\mu < -\mu^{-2}.$$

Recalling from Section 3 and Figures 3(a)–(c) that, for valid U-solutions, $u_c > u_a$ and $u_c > u_b$, and noting that $\alpha_1 > 0$, we deduce that

$$u_b - u_a > (u_c - u_a)/(1 + \mu\alpha_1) + (u_c - u_b)/\mu^2 > 0. \qquad \square$$

A combination of Lemmas 2 and 3 yields Theorem 1:

THEOREM 1. *Consider the class of travelling-wave solutions to Equations* (1)–(5)*, in which* μ *represents the gas mass flux,* λ *the solid heat capacity,* c *the wavespeed, whilst* u_a *and* u_b *represent the inlet and outlet temperatures. If the critical wavespeeds are defined as* $c_1 = \mu$ *and* $c_2 = \mu + \lambda$*, then:*

(i) *all travelling-wave solutions with* $c < c_1$ *satisfy* $u_b > u_a$*;*
(ii) *there are no bounded travelling-wave solutions which have* $c > c_2$*;*
(iii) *for* $c_1 < c < c_2$ *travelling-wave solutions for which* $u_b = u_a$ *may occur.*

The identification of a range of sufficiently slow wavespeeds ($c < \mu$) for which the outlet temperature always exceeds the inlet temperature is consistent with results of other authors [8], [10]. For such wavespeeds there is a net production of heat in the system; energy removal due to solid conversion is not strong enough to alter this balance.

CASE (B): $Q^+ > \mu > Q^- \geqslant 0$

In this case the appearance of two decaying modes in $x > 0$ and a single mode in $x < 0$ provides a degree of freedom not evident in our analysis thus far. This situation, with $Q^+ > \mu > Q^- > 0$, generalises that presented in [17], where travelling-wave solutions for which $U(\pm\infty) = u_a$ were studied, to include cases for which $u_b \neq u_a$. On the basis of the preceding sections, it is clear that this range of wavespeeds, with $c > \mu$, is the only situation for which solutions having $u_b = u_a$ are possible. By focusing attention on cases for which the up- and down-stream temperatures are equal, we now show that such solutions do indeed exist.

(Q,G)-solutions. For (Q,G)-solutions $Q^- = 0$ so that a unique wave speed $c = \lambda > \mu$ is realised. However, with B_1, B_2 and $A_1 \neq 0$ in Equations (27)–(29), the outlet temperature is not uniquely defined in terms of the control parameters. Thus, for each set of values of the control parameters λ, μ, u_a and u_c there exists a family of (Q,G) travelling-wave solutions, each having wavespeed $c = \lambda$, which are parameterised by u_b. The constraint $U(0) \geqslant u_c$ provides only a bound on the permissible range of outlet temperatures:

$$\mu < c = \lambda \leqslant 1 + \mu(u_b - u_a)/(u_c - u_b).$$

In Figure 7, for fixed values of μ and u_c, $(\lambda, U(0))$-space is partitioned into regions of existence of (Q,G)-solutions. The curve $u_b = u_a$, along which $U(0) = u_a + 1/\lambda$, separates domains

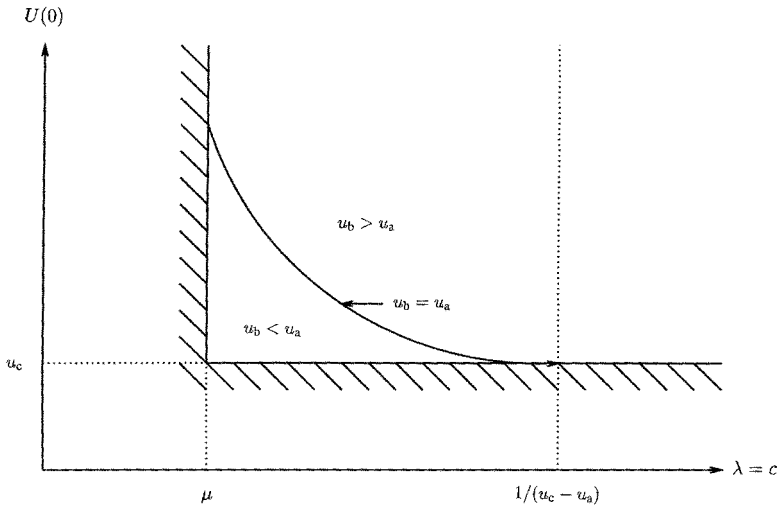

Figure 7. A schematic diagram showing the domain of existence of (Q,G)-solutions in $(\lambda, U(0))$ parameter-space. In addition to the control parameters u_a, u_c, μ and λ, solutions are parameterised by the outlet temperature u_b and their (uniquely determined) wavespeeds which satisfy $\mu < c = \lambda$. The region in which $u_b > u_a$ is separated from the region where $u_b < u_a$ by a curve along which travelling-wave solutions having equal inlet and outlet temperatures exist.

where $u_b < u_a$ and $u_b > u_a$. Asymptotic analysis in a neighbourhood of $u_b = u_a$ supplies the corresponding values of $U(0)$: for $0 < |\epsilon| \ll 1$, since $\lambda > \mu$,

$$\begin{aligned} u_b = u_a + \epsilon \;\Rightarrow\quad U(0) &= u_a + \lambda^{-1} + \epsilon(1 - \mu/\lambda), \\ \Rightarrow\; U_{\epsilon\neq 0}(0) &> U_{\epsilon=0}(0) \quad \text{if } \epsilon > 0, \\ &< U_{\epsilon=0}(0) \quad \text{if } \epsilon < 0. \end{aligned}$$

We remark that by fixing $u_b = u_a$ we obtain a unique (Q,G)-solution.

U-solutions. As for (Q,G)-solutions, with $A_1, B_1, B_2 \neq 0$ in Equations (27)–(29), it is no longer, in general, possible to define both c and u_b uniquely in terms of the control parameters λ, μ, u_a and u_c. With $u_b \neq u_a$, Equations (30) and (33) supply the following expression defining u_b in terms of the parameter $c \in (\lambda, \lambda + \mu)$:

$$u_b = u_a + (\lambda(u_c - u_a) - 1)/(c - \mu). \tag{40}$$

For the special case $\lambda = (u_c - u_a)^{-1}$, Equation (33) supplies $u_b = u_a$, independent of c, in which case there exists a family of U-solutions, all having $u_b = u_a$ and parameterised by the wavespeed $c \in (\lambda, \lambda + \mu)$. For fixed values of μ, u_a and u_c, Figure 8 shows how (λ, c)-space partitions into regions where $u_b > u_a$ and $u_b < u_a$, the curve $u_b = u_a$ separating them.

In the construction of Figure 8, asymptotic analysis again enables us to determine the sign of $u_b - u_a$ to the left/right of the curve $u_b = u_a$: for $0 < |\epsilon| \ll 1$, setting $\lambda = (u_c - u_a)^{-1} + \epsilon\lambda_1$ and $u_b = u_a + \epsilon$, Equation (40) supplies

$$c = \mu + \lambda_1(u_c - u_a) + O(\epsilon).$$

The above analysis demonstrates the existence of both (Q,G) and U-travelling waves for which $\mu < c < \mu + \lambda$, and provides our proof of Theorem 1, as stated in the introduction.

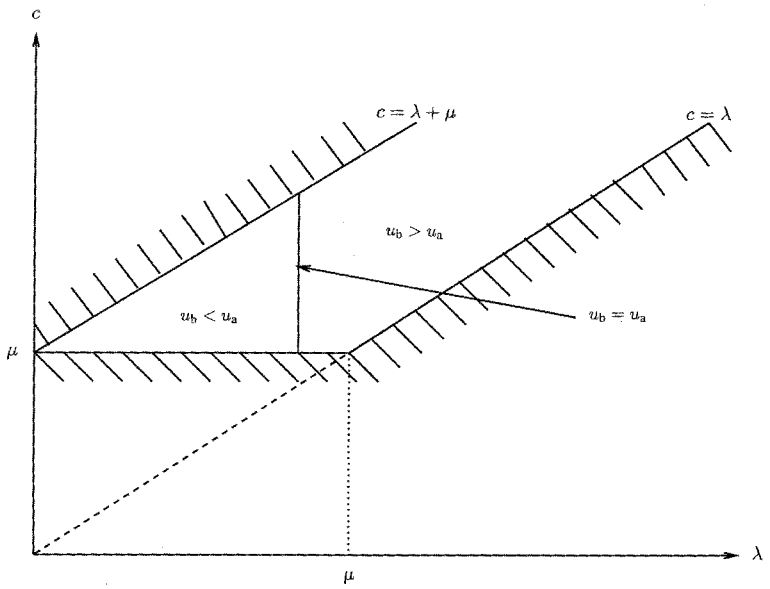

Figure 8. A schematic diagram showing the domain of existence of U-solutions in (λ, c) parameter-space. In addition to the parameters u_a, u_c, μ and λ, solutions are characterised by the wavespeed c which satisfies $\mu < c < \mu + \lambda$. The outlet temperature u_b is then defined in terms of u_a, u_c, μ, λ and c. As in Figure 7, the region in which $u_b > u_a$ is separated from the region where $u_b < u_a$ by a curve along which travelling-wave solutions having equal inlet and outlet temperatures exist.

Together with the analysis of Section 4, it also shows the crucial role played by the variable solid heat capacity in obtaining solutions for which $u_b = u_a$. The energy required to change the solid composition provides a sink for the energy produced by the chemical reaction, thereby restricting temperature growth and enabling travelling combustion wave with equal inlet and outlet temperatures to occur.

The degree of freedom in the wave speed experienced by U-solutions is reminiscent of work in [11], [26]. We expect that, in practice, the wave speed will attain a unique value. To determine this speed, further study is needed. For example, a time-dependent stability analysis, such as that described in [18], may indicate that the relevant, stable wavespeed corresponds to the slowest value in the feasible range. The degree of freedom experienced by (Q,G)-solutions is new: in this case, the wavespeed is specified, whilst the outlet temperature is not well-defined. Again, further study is needed to determine the unique outlet temperature that would be observed in practice.

Similarities with the work in [11], [26] highlight an important difference between the work described here and that of [17]. Working with a finite-length reaction zone over the same range of wave-speeds ($Q^+ > \mu > Q^- > 0$), and assuming that $u_b = u_a$, Norbury and Stuart obtained unique travelling-wave solutions whereas, here, with a delta-function reaction rate, we obtain non-unique solutions, the degeneracy arising from an ill-defined wavespeed for U-solutions and an ill-defined outlet temperature for (Q,G)-solutions. Thus, if we follow [17] and specify $u_b = u_a$ then we recover a unique (Q,G)-solution, whereas the U-solution remains ill-defined. We believe that this discrepancy arises in the limit when the finite-length, finite-strength reaction rate approaches the delta-function rate. In the limit, the distinct solutions

obtained for the finite-length reaction rate coalesce, giving rise to a degenerate solution. This difference will be the subject of further study.

Appendix

In this appendix the stabilising effect of including solid-conversion effects ($\lambda > 0$) is examined through a preliminary linear stability analysis of the travelling-wave solutions discussed in the main text. Perturbations to only the solid- and gas-temperature profiles are considered, with the underlying steady solutions balancing fully the delta-function reaction term, and the inlet/outlet boundary conditions remaining fixed. We assume further that the perturbations are, at least initially, spatially bounded and focus on their temporal behaviour – do they grow with time, indicating instability? For simplicity, only two limiting cases are considered:

- (I) $\lambda = 0 \quad \Rightarrow \sigma \equiv 1 \; \forall \; x \in (-\infty, \infty)$,
- (II) $\lambda = c > 0 \quad \Rightarrow \sigma = 1$ for $x \in (0, \infty)$ and $\sigma = 0$ for $x \in (-\infty, 0)$.

The analysis presented for these cases generalises naturally when $\lambda \in (0, c)$.

For case (I), where no solid conversion takes place, we show that only G-solutions possess perturbations of the type being considered and that these perturbations are stable. We then show how the inclusion in case (II) of $\lambda > 0$ gives rise to not just stable G-solutions, but also stable Q-solutions.

Recalling the original time-dependent Equations (1)–(5), we seek solutions of the form

$$\begin{aligned} u(z,t) &= U(x) + \mathrm{e}^{\theta t}\bar{u}(x), \quad (0 < |\bar{u}| \ll |U|) \\ w(z,t) &= W(x) + \mathrm{e}^{\theta t}\bar{w}(x), \quad (0 < |\bar{w}| \ll |W|) \\ c\sigma(z,t) &= Q(x), \\ g(z,t) &= G(x), \end{aligned}$$

where $x = z - ct$ is the travelling-wave coordinate and stability of the solution depends upon the real part of θ being positive. The dependent variables (U, W, Q, G) satisfy Equations (6)–(12), (14) whilst the perturbations $(\bar{u}, \bar{w})$ satisfy

$$0 = \bar{u}'' + c\sigma\bar{u}' + \bar{w} - (1+\theta)\bar{u}, \tag{41}$$

$$\mu\bar{w}' = \bar{u} - \bar{w}, \tag{42}$$

subject to

$$\bar{u}(\pm\infty) = \bar{u}'(\pm\infty) = \bar{w}(\pm\infty) = 0. \tag{43}$$

In deriving Equation (41) we assume that the effect of the reaction rate is fully absorbed by the steady travelling-wave solutions and hence that $\bar{u}, \bar{u}', \bar{w}$ are continuous across the flame front ($x = 0$). In addition, for valid solutions we assume that, at $t = 0$, $\bar{u}(x = 0)$ is such that $U(x = 0) + \bar{u}(x = 0) \geqslant u_{\mathrm{c}}$. Equations (41)–(43) are solved below for the cases $\lambda = 0$ and $\lambda = c$.

Case (I). With $\sigma \equiv 1$ Equations (41)–(43) integrate to give

$$\bar{u}(x) = \begin{cases} \sum_{i=1}^{3} A_i \, \mathrm{e}^{-\gamma_i x} & \text{if } x < 0, \\ \sum_{i=1}^{3} B_i \, \mathrm{e}^{-\gamma_i x} & \text{if } x > 0. \end{cases} \tag{44}$$

$$\bar{w}(x) = \begin{cases} \sum_{i=1}^{3} A_i(1-\mu\gamma_i)^{-1}\,\mathrm{e}^{-\gamma_i x} & \text{if } x < 0, \\ \sum_{i=1}^{3} B_i(1-\mu\gamma_i)^{-1}\,\mathrm{e}^{-\gamma_i x} & \text{if } x > 0. \end{cases} \tag{45}$$

where $\{A_i, B_i\}$ are constants of integration, and $\{\gamma_i\}$ are roots of the cubic

$$0 = \mu\gamma^3 - (1+\mu c)\gamma^2 - (\mu - c + \theta\mu)\gamma + \theta. \tag{46}$$

Thus, for bounded initial data, we fix $A_i = 0$ if $\Re(\gamma_i) > 0$ and $B_i = 0$ if $\Re(\gamma_i) < 0$. For fixed values of μ and c, as the eigenvalue θ varies, different cases arise according to the number of roots of (46) possessing positive, and negative, real parts. We show below that stable perturbations for G-solutions do exist, whereas no solutions are possible for U-solutions.

Cases for which the roots of (46) have real parts of the same sign can be rejected immediately. For example, if $\Re(\gamma_i) > 0$ $(i = 1, 2, 3)$, then $\bar{u} = 0 = \bar{w}$ in $x < 0$. Since the proposed solutions are infinitely differentiable, continuity of $\bar{u}, \bar{u}', \bar{w}$ across $x = 0$ implies also that $\bar{u}''(x = 0) = 0$, so that $\bar{u} = 0$ in $x > 0$ and no nontrivial perturbations exist.

Suppose, then, that (46) possesses two positive and one negative real roots. Without loss of generality, the coefficients A_1, B_2 and B_3 are given by

$$A_1 = B_2 + B_3, \qquad \gamma_1 A_1 = \gamma_2 B_2 + \gamma_3 B_3, \qquad \frac{A_1}{1-\mu\gamma_1} = \frac{B_2}{1-\mu\gamma_2} + \frac{B_3}{1-\mu\gamma_3}.$$

The first pair of equations provide expressions for B_2, B_3 in terms of A_1

$$B_2 = (\gamma_3 - \gamma_1)/(\gamma_3 - \gamma_2)A_1, \qquad B_3 = (\gamma_2 - \gamma_1)/(\gamma_2 - \gamma_3)A_1.$$

Substitution with these expressions in the third equation, assuming a nontrivial solution ($A_1 \neq 0$), yields the following consistency condition

$$(\gamma_3 - \gamma_2)/(1-\mu\gamma_1) = (\gamma_3 - \gamma_1)/(1-\mu\gamma_2) - (\gamma_2 - \gamma_1)/(1-\mu\gamma_3),$$

which has solutions $\gamma_3 = \gamma_2, \gamma_1 = \gamma_2$ and $\gamma_1 = \gamma_3$. Since $\gamma_1 < 0 < \gamma_2, \gamma_3$, only $\gamma_3 = \gamma_2$ is possible: (46) possesses a repeated root, and we consider trial solutions of the form $\bar{u} = (B_1 + B_2 x)\,\mathrm{e}^{-\gamma_2 x}$ in $x > 0$. Now identities relating the sum and product of the roots of (46) when $\gamma_2 = \gamma_3$ yield three relations from which θ, c and γ_1 can be determined in terms of μ and γ_2. After some rearrangement, we deduce

$$\gamma_1 = \mu^{-1} + \mu/(1-\mu\gamma_2)^2 > 0,$$

which contradicts $\gamma_1 < 0$. Hence, no solutions of this form may occur. Similar arguments exclude the case for which γ_2, γ_3 are a complex conjugate pair with positive real parts.

Finally, suppose that (46) has three real roots $\gamma_1 \leqslant \gamma_2 < 0 < \gamma_3$. As above we deduce that $\gamma_2 = \gamma_1 < 0$ and

$$\gamma_3 = \mu^{-1} + \mu/(1-\mu\gamma_2)^2 > 0.$$

Recalling that $\sigma \equiv 1$, we remark that only G-solutions (for which $a = \mu$) and U-solutions can occur. For U-solutions $\bar{u}(x = 0) = 0$ so that $A_1 = A_2 = B_3 = 0$ and no nontrivial perturbations exist. For G-solutions this restriction does not apply and we obtain perturbations of the required form. Recalling that $0 < \Pi_{i=1}^{3}\gamma_i = -\theta/\mu$, we remark further that $\theta < 0$

and, hence, that these perturbations are stable. Similar analysis yields stable G-solutions when γ_1, γ_2 are complex conjugates with negative real parts.

Case (II). With $\sigma = 1$ in $x > 0$ and $\sigma = 0$ in $x < 0$, Equations (41)–(43) integrate to give

$$\bar{u}(x) = \begin{cases} A\,\mathrm{e}^{\phi x} & \text{if } x < 0, \\ \sum_{i=1}^{3} B_i\,\mathrm{e}^{-\gamma_i x} & \text{if } x > 0. \end{cases} \tag{47}$$

$$\bar{w}(x) = \begin{cases} A(1+\phi\gamma_i)^{-1}\,\mathrm{e}^{\phi_i x} & \text{if } x < 0, \\ \sum_{i=1}^{3} B_i(1-\mu\gamma_i)^{-1}\,\mathrm{e}^{-\gamma_i x} & \text{if } x > 0. \end{cases} \tag{48}$$

where $\phi > 0$ satisfies

$$0 = \phi^2 + \mu^{-1}\phi - 1.$$

As for case (I), $\{\gamma_i\}$ are the roots of (46), and the constants of integration $A, \{B_i\}$ are determined by imposing continuity of $\bar{u}, \bar{u}', \bar{w}$ across $x = 0$. Following case (I), we see that the cases which yield nontrivial perturbations correspond to (46) possessing one, two or three roots with positive real parts.

If we assume a single positive real root, then continuity of $\bar{u}, \bar{u}', \bar{w}$ across $x = 0$ supplies

$$A = B_1, \qquad \phi A = -\gamma_1 B_1, \qquad A(1+\mu\phi)^{-1} = B_1(1-\mu\gamma_1)^{-1},$$
$$\Rightarrow A = B_1 = 0 \quad (\text{since } \phi \neq -\gamma_1).$$

Hence no nontrivial perturbations can occur. Similarly, no valid perturbations exist when (46) possesses two roots with positive real parts, the analysis mimicking exactly that presented for case (I). Thus the only possibility arises when all roots of (46) have positive real parts. For example, if we assume three positive real roots, then continuity of $\bar{u}, \bar{u}', \bar{w}$ across $x = 0$ supplies three equations from which $\{B_i\}$ are determined in terms of $A, \mu, \phi, \{\gamma_i\}$. Further, $\theta/\mu = -\Pi\gamma_i \;\Rightarrow \theta < 0$, so that such perturbations are stable. Finally, for nontrivial perturbations, $\bar{u}(x = 0) \neq 0$, so that these results refer only to Q-solutions or G-solutions, not U-solutions.

In summary, in this preliminary stability analysis, we have shown that gas-fuel- and solid-fuel-limited travelling-wave solutions are stable with respect to a certain class of perturbation. For U-solutions, no such nontrivial perturbations could be found. This is due to the restrictive nature of the perturbations considered. A perturbation of the solid and gas temperatures alone supplies extra energy to the system. For the solid- and gas-fuel limited solutions, this additional energy is used to change the solid/gas properties, giving rise to a modified temperature at the flame front ($x = 0$). However, for the U-solution, there is no means by which the energy can redistribute itself, the temperature at the front, the inlet and the outlet being held fixed. Relaxation of, for example, the wavespeed or the boundary conditions could resolve this issue. Such modifications will form the basis of a more detailed stability analysis of the travelling-wave solutions discussed in this paper. However, the stability of the gas- and solid-fuel-limited travelling waves is consistent with the stability results in [18].

References

1. M.F.R. Mulcahy and I.W. Smith, Kinetics of combustion of pulverised fuel: a review of theory and experiment, *Rev. Pure and Appl. Chem.* 19 (1969) 81–108.

2. A.A Butakov, E.I. Maksimov and K.G. Shkadinsky, Theory of chemical displacement reactors. *Comb. Expl. Shock Waves* 14 (1978) 48–54.
3. N.M. Chechilo and N.S. Enikolopyan, Structure of the polymerization wave front and propagation mechanism of the polymerization reaction. *Dokl. Phys. Chem.* 214 (1974) 164-176.
4. J.D. Buckmaster and G.S.S. Ludford, *Theory of Laminar Flames*, Cambridge: Cambridge University Press (1982) 266pp.
5. D.A. Frank-Kamenetskii, *Diffusion and Heat Transfer in Chemical Kinetics*, New York: Plenum Press (1969) 370pp.
6. F.A. Williams, Theory of combustion in laminar flows, *Annual Rev. Fluid Mech.* 3 (1971) 171–188.
7. V.S. Babkin, V.I. Drobyshevich, Y.M Laevskii and S.I. Potynyakov, Filtration combustion of gases, *Combustion, Explosion and Shock Waves* 19 (1983) 17–26.
8. P.C. Fife, Propagating fronts in reactive media. In: A. Bishop, D. Campbell and B. Nicolaenko (eds), *Nonlinear Problems: Present and Future*. Mathematical Studies 61 (1982) pp. 267–285.
9. O.V. Kiselev and V.S. Matros, Propagation of the combustion front of a gas mixture in a granular bed of catalyst, *Combustion, Explosion and Shock Waves* 16 (1980) 25–30.
10. B.J. Matkowsky and G.I. Sivashinsky, Propagation of a pulsating front in solid fuel combustion, *SIAM J. Appl. Math.* 35 (1978) 465–478.
11. YA. B. Zeldovich, G.I. Barenblatt, V.B. Librovich and G.M. Makhviladze, *The Mathematical Theory of Combustion and Explosions*. New York: Consultants Bureau, Plenum (1985) 597pp.
12. H.M. Byrne, *Modelling Combustion Zones in Porous Media*. D. Phil. Thesis, Oxford University (1991) 176pp.
13. H. Byrne, Travelling combustion waves in porous media. In: F. Hodnett (ed.), *Proceedings of the Sixth European Conference on Mathematics in Industry*. B.G. Teubner Stuttgart (1992) pp. 99–102.
14. H. Byrne and J. Norbury, Mathematical modelling of catalytic converters, *Math. Engng. Ind.* 4 (1993) 27–48.
15. H. Byrne and J. Norbury, Stable solutions for a catalytic converter, *SIAM J. Appl. Math.* 54 (1994) 789–813.
16. D.A. Lawson and J. Norbury, Numerical solution of combustion in a porous medium. In: R.W. Lewis *et al.* (eds), *Numerical Methods in Heat Transfer*, Vol. III. Chichester: John Wiley (1985) pp. 175–181.
17. J. Norbury and A.M. Stuart, Travelling combustion waves in a porous medium, Part I – Existence, *SIAM J. Appl. Math.* 48 (1988) 155–169.
18. J. Norbury and A.M. Stuart, Travelling combustion waves in a porous medium, Part II – Stability, *SIAM J. Appl. Math.* 48 (1988) 374–392.
19. J. Norbury and A.M. Stuart, A model for porous medium combustion, *Quart. J. Mech. and Appl. Math.* 42 (1989) 159–178.
20. J.W. Hightower, Catalytic converters for motor vehicles: general overview, *A.I.Ch.E. Symp. Ser.* 72 (1976) 354–368.
21. M.R. Booty and B.J. Matkowsky, On the stability of counter flow filtration combustion, *Combustion, Science and Technology* 80 (1991) 231–264.
22. M.R. Booty and B.J. Matkowsky, Modes of burning in filtration combustion, *European Journal of Applied Mathematics* 2 (1991) 17–41.
23. A. Egerton, K. Gugan and F.J. Weinberg, The mechanism of smouldering in cigarettes, *Combustion and Flame* 7 (1963) 63–78.
24. T.J. Ohlemiller and D.A. Lucca, An experimental comparison of forward and reverse smolder propagation in permeable fuel beds, *Combustion and Flame* 54 (1983) 131–147.
25. G.C. Bond, *Heterogeneous Catalysis: Principles and Applications* (2nd ed.) Oxford: Clarendon Press (1987) 176pp.
26. K.K. Tam, Travelling wave solutions for a combustion problem, *Stud. in Appl. Math.* 81 (1989) 117–124.
27. H. Berestycki, B. Nicolaenko and B. Scheurer, Travelling wave solutions to reaction diffusion systems modelling combustion, *Contemporary Math.* 17 (1983) 189–207.
28. S.H. Oh and J.C. Cavendish, Transients of monolithic catalytic converters: response to step-change in feedstream temperature as related to controlling automobile emissions, *Ind. Eng. Chem. Res. Dev.* 21 (1982) 29–37.